Received: 9 July 2020 | Revised: 30 September 2020 | Accepted: 22 November 2020

DOI: 10.1002/app.50361

ARTICLE

Applied Polymer SCIENCE WILEY

Ionic liquid gated poly(triaryl amine) thin film field effect transistor

Luis M. Rijos[1] | **Kelotchi S. Figueroa**[1] | **Angelo Porcu**[1] | **Naomi M. Rivera**[2] | **Anamaris Meléndez**[1] | **Idalia Ramos**[1] | **Nicholas J. Pinto**[1]

[1]Department of Physics and Electronics, University of Puerto Rico at Humacao, Humacao, Puerto Rico

[2]Department of Chemistry, University of Puerto Rico at Humacao, Humacao, Puerto Rico

Correspondence
Nicholas J. Pinto, University of Puerto Rico, Physics and Electronics, 100 Road#908, Humacao 00791, Puerto Rico.
Email: nicholas.pinto@upr.edu

Funding information
National Science Foundation (US), Grant/Award Number: 1800262; National Science Foundation (US), Grant/Award Number: 1523463

Abstract

A poly(triaryl amine) thin film field effect transistor was investigated in air with ionic liquid (IL) gating for the first time. The transistor retained a high-on/off ratio of ~700 and mobility of $\sim 10^{-2}$ cm^2/V-s. When compared to a transistor based on the conducting polymer polyaniline under similar operating conditions, it was found to exhibit superior performance. Significantly low-operating voltages (±1 V) enhances the possibility of its use in organic electronics. The device was successfully tested for binary operation, and we demonstrate its suitability for use in low-power consumption electronic circuits.

KEYWORDS

FET, conducting polymers, ionic liquids, polyamides

1 | INTRODUCTION

The discovery of π conjugated poly-acetylene in 1997 led to a new field of conducting polymers and subsequently toward plastic electronics beginning in the 1980's.[1–4] Although they were initially unstable and decomposed under ambient conditions, a variety of next generation *p*- and *n*-type polymers are now commercially available that are air stable.[5–7] The charge mobility in some polymers is comparable to or higher than that of amorphous silicon and can replace it in applications where flexibility is needed. An advantage of using conducting polymers over silicon is that they are relatively inexpensive to synthesize, and devices can be fabricated under ordinary laboratory conditions without the use of a clean room facility. Poly (triaryl amine)–PTAA, that is, poly[bis(4-phenyl) (2,4,6-trimethylphenyl)amine] is one such commercially available undoped hole transporting (*p*-type) semiconducting polymer that is easily processable, and promising for photovoltaic applications.[8–13] Although it is air stable and its amorphous nature and nonplanarity lead to smooth film formation upon spin coating, there often exist charge traps at the polymer/substrate interface due to substrate roughness. This lowers the mobility due to scattering and necessitates high-operating voltages.[8,10–12,14] The importance of this manuscript is that we overcome this limitation by using an ionic liquid (IL) as the gate insulator in a field effect transistor (FET) configuration. We show that the operating voltages can be as low as ~ ±1 V while retaining an on/off ratio ~ 700 and saturated hole mobility $\sim 10^{-2}$ cm^2/V-s. By applying a pulsed signal input, the device was tested with different drain-source (V_{DS}) voltages. A significant output was recorded only when the input voltage was biased negative with respect to the source, consistent with the *p*-type nature of PTAA. Our device performance was compared to that fabricated

using doped polyaniline[15] and found to have superior parameters. This is the first report on a PTAA thin film FET gated with an IL and demonstrates a technique of using it as an alternative in low-power consumption organic devices.

2 | EXPERIMENTAL DETAILS

Poly[bis(4-phenyl)(2,4,6-trimethylphenyl)amine]-PTAA was purchased from Millipore Sigma and used as received. 15 mg of PTAA was dissolved in 1 ml of chlorobenzene and spin coated (2000 rpm, 45 s) on to a prepatterned Si^+/SiO_2 substrate. The substrate was then placed in an oven at 70°C for 12 h. The average film thickness was ~60 nm. Figure 1(a) shows the molecular structure of PTAA. It is nonplanar with a large linkage angle resulting in an amorphous microstructure that limits mobility. For the IL, a 9 wt% of 1-ethyl-3-methylimidazolium bis (triflurometh ylsulfonyl) imide–$(EMI)^+(TFSI)^-$ (0.135 g) and 1 wt% of poly(styrene-b-methyl methacrylate-b-styrene) triblock copolymer-SMS-15-81-15 (0.015 g) was dissolved in 90 wt% of methylene chloride (1.35 g) to form a clear solution.[16,17] We chose this IL because it is commercially available, it has a wide electrochemical window and because it has a high-specific capacitance. To increase its viscosity prior to use, the IL was placed in an oven at 70°C for several hours. Figure 1(b) shows the molecular structure of the IL.

Figure 2(a) shows a top view optical microscope image of the prepatterned Si^+/SiO_2 substrate prior to spin coating it with PTAA. The inset to this figure shows a magnified view of the closely spaced prepatterned Au electrodes. Two adjacent electrodes eventually become the source (S) and drain (D) terminals of the device. The spacing (L) between electrodes was 3 μm and the width (W) of the electrode was 475 μm. Figure 2(b) shows the same substrate as in Figure 2(a) after spin coating it with PTAA and annealing. The inset to this Figure shows a high-magnification scanning electron microscope (SEM) image on a scratched surface of the device. The surface of the PTAA film is very smooth as seen when contrasted to the bare SiO_2 surface. Figure 2(c) shows the IL placed over the substrate seen in Figure 2(b) that covered the polymer between the S and D terminals. A thin Au wire inserted into the IL served as the gate (G) electrode. Figure 2(d) shows a schematic of the device together with the external electrical connections. All measurements were conducted in air at room temperature and in the dark. A Keithley electrometer model 6517B provided the drain-source voltage (V_{DS}) and recorded the drain-source current (I_{DS}), while a Keithley model 2400 source meter provided the gate-source voltage (V_{GS}). The source

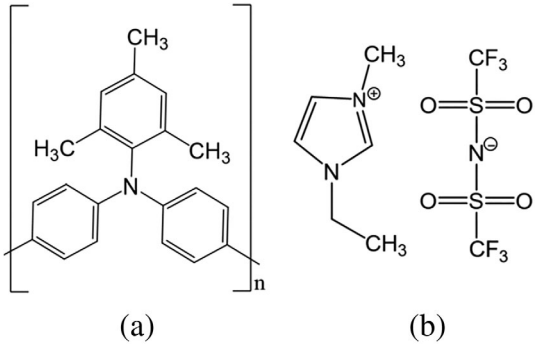

FIGURE 1 Chemical structures of (a) poly(triaryl amine)-PTAA (i.e., poly[bis(4-phenyl)(2,4,6-trimethylphenyl)amine) and (b) the ionic liquid 1-ethyl-3-methylimidazolium bis (triflurometh ylsulfonyl) imide – $(EMI)^+(TFSI)^-$

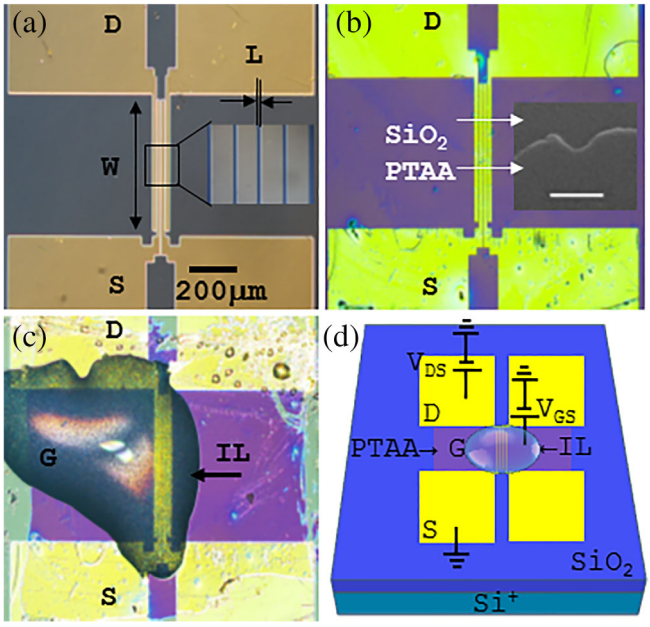

FIGURE 2 (a) Top view optical microscope image of the Si^+/SiO_2 substrate with prepatterned Au electrodes. The inset shows a magnified section where the electrode separation is 3 μm. Two closely spaced electrodes are labeled S and D for the source and drain terminals, respectively. L and W represent the length and width of the semiconducting channel respectively. (b) Same substrate as in (a) but with a spin coated thin film of PTAA. The inset to this figure is a high-magnification SEM image on a scratched surface of the device. The surface of the PTAA film is very smooth as seen when contrasted to the bare SiO_2 surface. The scale bar in this inset is 1 μm. (c) Same substrate as in (b) but with an IL drop cast over the S/D channel. A wire inserted into the IL acts as the gate (G) electrode. (d) Schematic diagram of the device with the external electrical connections. IL, ionic liquid; PTAA, poly (triaryl amine); SEM, scanning electron microscope [Color figure can be viewed at wileyonlinelibrary.com]

terminal was used as the common ground. Since PTAA is a *p*-type polymer, the device was characterized in the third quadrant of the I_{DS}-V_{DS} plot to enhance hole transport.[18] In all of the measurements, the gate voltage was swept at a rate of 20 mV/s. Impedance spectroscopy was carried out in air using an Agilent 4294A impedance analyzer, while the film thickness was measured using a KLA Tencor D-500 profilometer. A JEOL SEM was used to study the PTAA film topography.

3 | RESULTS AND DISCUSSION

The IL was first characterized *via* impedance spectroscopy to determine the specific capacitance and to confirm charge doping (as opposed to chemical doping) when used in the devices under study. Using a parallel plate capacitor filled with the IL, the specific capacitance (C_i) of the IL was measured as a function of frequency and plotted in Figure 3(a). The inset Figures in this plot shows a photograph of the actual capacitor and the schematic diagram with external connections. The capacitor spacing was ~100 μm. The inability of the heavy ions in the IL to follow the alternating electric field at high-frequencies lead to a decrease in C_i, while at low frequencies it was relatively constant and approached ~13 μF/cm^2. For comparison, the specific capacitance of a 150 nm thick SiO_2 layer was ~20 nF/cm^2.[19] A large specific capacitance is the primary reason for the low-operating voltages in the device (as seen later) since the voltage drop across the IL is small and a large fraction of the applied voltage appears directly at the IL/polymer interface. Figure 3(b) shows the dependence of specific capacitance of a metal–insulator-Si^+ device with a DC bias superimposed on the 10 mV exciting AC frequency. A positive(negative) bias applied to the IL would direct the cations (anions) toward the IL/Si^+ interface. The MIS structure (inset) mimics the PTAA device studied here and assists in data interpretation. As seen in Figure 3(b), at a preselected frequency, C_i increases as the DC bias was made more negative indicating hole accumulation in Si^+ due to the presence of anions at the IL/Si^+ interface. A positive DC bias depletes the holes and reduces the capacitance. Overall, C_i was reduced for higher frequencies and was relatively constant for negative DC voltages similar to previous reports.[19] This constant capacitance at negative bias suggests charge injection into the Si^+ semiconductor (as opposed to chemical doping) at the semiconductor/IL interface.[20]

Figure 4(a) shows the I_{DS} versus V_{DS} curves of the PTAA device seen in Figure 2(c) for various gate voltages V_{GS}. In this figure, V_{GS} was first set to −1.0 V and slowly increased to +1.0 V in steps of +0.1 V. At each V_{GS}, the device I_{DS} was recorded as a function of V_{DS}. Four important features of this plot are: (i) the super linear Ohmic I_{DS}-V_{DS} curve at low V_{DS} (< 0.1 V) suggest the absence of Schottky barriers at the polymer/metal interface. This is because Au and PTAA have almost identical energy level bands, that is, the Fermi level in Au and the HOMO level in the polymer are similar.[14] It is also possible that surface states in PTAA cause Fermi energy pinning at the Au/PTAA interface, which is not affected by the IL. (ii) The channel currents decrease as the gate voltage is made more positive and vice versa. This is consistent with the *p*-type nature of PTAA.[10] (iii) At each fixed gate voltage, a clear saturation is observed in the current as V_{DS} is increased, confirming that the device operates as a true FET. (iv) The operating voltages are significantly smaller compared to other PTAA based FET's.[10] The constant specific capacitance at low frequency when the gate voltage is negative (Figure 3(b)) indicate electrostatic charge doping *via* hole injection into the PTAA channel.[20] Under these conditions, according to the standard FET theory, the channel current (I_{DS}) dependence on the gate voltage for fixed V_{DS} is given by[21]:

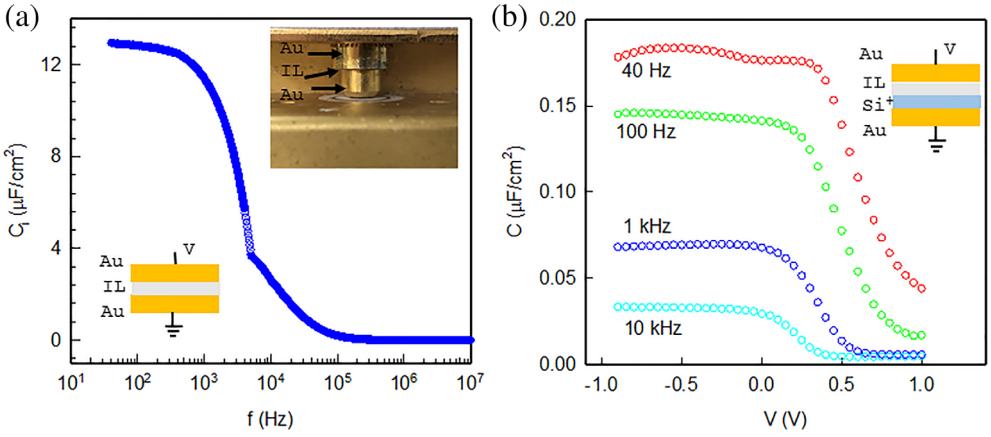

FIGURE 3 (a) Ionic liquid specific capacitance as a function of frequency using the capacitor configuration shown in the inset. (b) Si^+/IL specific capacitance as a function of applied DC voltage superimposed on a 10 mV AC exciting voltage. The device schematic is shown in the inset. IL, ionic liquid [Color figure can be viewed at wileyonlinelibrary.com]

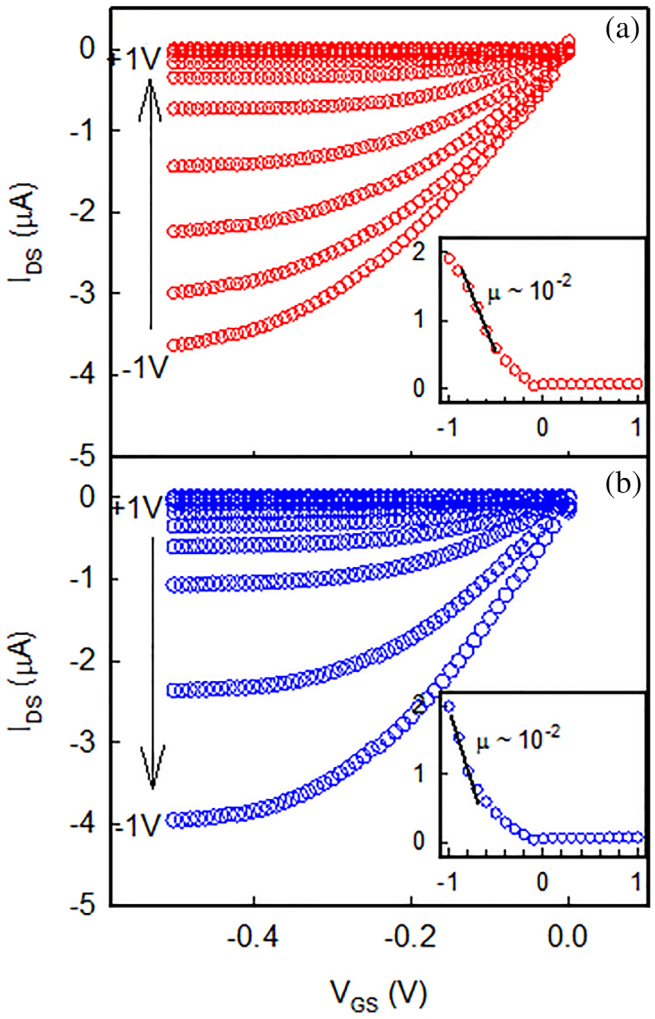

FIGURE 4 (a) Drain-source current (I_{DS}) versus drain-source voltage (V_{DS}) for top gate voltage (V_{GS}) scan from –1 V → +1 V in steps of 0.1 V. The inset is a plot of $\sqrt{|I_{DS}|}$ vs.V_{GS} at fixed $V_{DS} = -0.5$ V. This data is extracted from the main figure. (b) Drain-source current (I_{DS}) versus drain-source voltage (V_{DS}) for top gate voltage (V_{GS}) scan from +1 V → -1 V in steps of −0.1 V. The inset is a plot of $\sqrt{|I_{DS}|}$ vs.V_{GS} at fixed $V_{DS} = -0.5$ V. This data is extracted from the main figure. The plots in the insets are used to calculate the mobility (μ) [Color figure can be viewed at wileyonlinelibrary.com]

$$I_{DS} = \frac{\mu W C_i (V_{GS} - V_{TH})^2}{2L}, \quad (1)$$

where μ is the charge mobility, C_i is the IL specific capacitance (13 μF/cm^2) and V_{TH} is the threshold voltage for the onset of channel current (i.e., below this voltage the channel is pinched off). In the saturation regime ($V_{DS} = -0.5$ V), the charge mobility can be calculated from the data shown in the inset to Figure 4(a). In this plot, the square root of the absolute values of the currents at $V_{DS} = -0.5$ V are plotted versus the corresponding gate voltages. Using Equation (1), the mobility was extracted from the slope of the linear section of this plot as indicated with the straight line and calculated to be 1.0 x 10^{-2} cm^2/V-s. Figure 4(b) shows similar plots for the device, however, in this figure the gate voltage is changed from +1.0 V to −1.0 V in steps of −0.1 V. The plots have qualitatively similar features to that seen in Figure 4(a), the calculated mobility however is seen to be 2.4 x 10^{-2} cm^2/V-s. These values are consistent with previous measurements[10,22] and represent a lower limit since the actual gate voltage at the IL/PTAA interface would be smaller due to the finite IL conductivity. Figures S3, S4 and S5 in the supplementary section show similar results of I_{DS} versus V_{GS} for a new device when a reference electrode is inserted into the IL for more accurate voltage measurements. A higher mobility in the gate scan from +1.0 V → -1.0 V compared to the scan from −1.0 V → +1.0 V could be due to the slow turning on of the device from the off state, a process where charge traps can be filled thereby reducing scattering. The threshold voltage for the onset of channel current as seen in the inset plots to Figure 4 is ∼ −0.15 V. The average device I_{on}/I_{off} ratio measured using the data in Figures 4 at $V_{DS} = -0.5$ V for $V_{GS} = -/+ 1$ V was ∼700. This value is small compared to other reports,[10] however, the operating voltages in our device are significantly lower in comparison and hence suitable for low-power consumption electronics. The IL conductivity did not adversely affect our device performance. We fabricated and tested a new PTAA-FET with back (SiO_2) gating and top (IL) gating on the same PTAA channel. The device was electrically characterized with the back gate first (no IL placed on the channel) and then with the top IL gate (no back gate bias). The results are plotted in Figures S1 and S2 in the supplementary section and show superior device performance with the IL gate when compared to the SiO_2 gate. As seen in Figure S2, the gate leakage currents were much smaller than the PTAA channel currents and assist our explanation of the observed data. It also strengthens the reliability of the parameters calculated above.

The device was further characterized by dynamically measuring the trans-conductance. In this measurement, V_{DS} was held fixed at −0.5 V while V_{GS} was varied as follows: -1 V → +1 V → -1 V in steps of 0.01 V and I_{DS} was measured. The difference in this measurement compared to that used to obtain data plotted in Figure 4 is that V_{DS} was fixed and not allowed to vary at any point during the measurement. Figure 5 shows the semi-log plot of the absolute value of I_{DS} versus V_{GS}. The data are consistent with that obtained in Figure 4, that is, a positive gate voltage reduced the channel current while a negative gate voltage increased it. The currents were slightly lower compared to that recorded in Figures 4. The average charge mobility calculated from the straight line sections

of this plot is 1.4 x 10^{-3} cm^2/V-s, while the threshold voltage is seen to be ~ +0.15 V. These values differ slightly from those extracted from Figure 4. In Figures 4 V_{GS} was fixed and V_{DS} was varied, while in Figure 5, V_{DS} was fixed and V_{GS} was varied. Having a fixed V_{GS} applies a stress to the IL over a longer time interval allowing a larger fraction of the ions to reach the IL/PTAA interface. This shifts the threshold voltage in a direction toward the applied gate voltage, consistent with previous results.[14] Since the gate voltage was changing during the measurement in Figure 5, the currents are slightly lower as the ionic response to the changing electric field due to the gate voltage was slow. A slower gate scan rate should result in higher currents. The sub-threshold swing (SS) in this device as measured from the semi-log plot of Figure 5 is 370 mV/decade, which is reasonably close to the ideal value of 66 mV/decade[23] for FET's. An additional advantage of applying a top gate voltage is that it minimizes detrimental effects of substrate roughness and charge traps at the SiO_2/polymer interface. Table 1 compares the transistor parameters of PTAA to that fabricated using the most widely studied conducting polymer polyaniline having the same architecture and under similar operating conditions.[15] Overall we see that PTAA is a superior polymer when compared to polyaniline for semiconducting applications, that is, increased on/off ratio, mobility and a low-threshold voltage. Several PTAA devices were studied with IL gating and yielded qualitatively similar results to that reported here. The devices stayed operational in air for approximately 2 weeks after which the measured currents were small and unreliable. One possible reason is an acidic decomposition of the IL that irreversibly interacts with PTAA. An XRD analysis of the device would provide better insight into any PTAA/IL interaction. Operating the device in a vacuum could extend this time period.

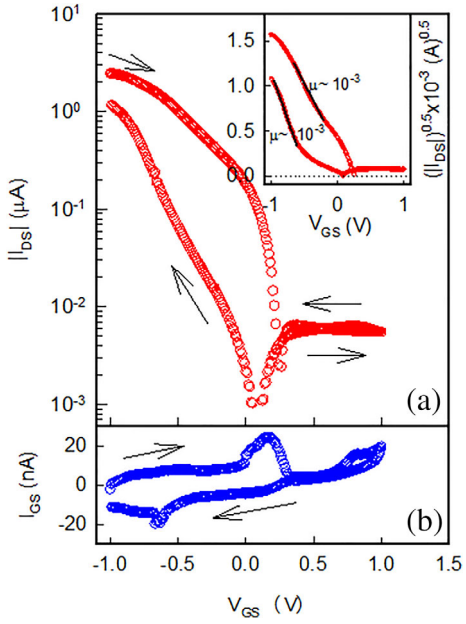

FIGURE 5 (a) Absolute value of the drain-source current (I_{DS}) as a function of gate-source voltage (V_{GS}) for fixed drain-source voltage (V_{DS}) of −0.5 V plotted on a semi-log scale. Inset: $\sqrt{|I_{DS}|}$ *vs.* V_{GS} using the data in the main figure. Approximate mobility values are shown next to the straight line portions of the plot. (b) Gate-source current (I_{GS}) as a function of V_{GS} for a fixed V_{DS} of −0.5 V [Color figure can be viewed at wileyonlinelibrary.com]

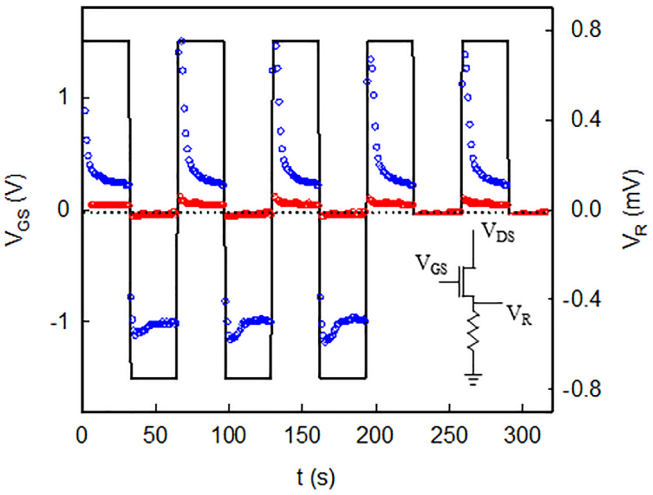

FIGURE 6 Pulsed response of the PTAA device showing the input and output voltages as a function of time. The input gate voltage (V_{GS}) was switched between ±1.5 V, and the output response (V_R) tapped across the 10 kΩ resistor for different values of the drain-source voltage (V_{DS}): Red: V_{DS} = 0 V; blue: V_{DS} = −2 V. PTAA, poly (triaryl amine) [Color figure can be viewed at wileyonlinelibrary.com]

TABLE 1 Comparison of device parameters of PTAA and polyaniline[14] when used in a thin film FET configuration with an ionic liquid gate. V_{TH} = threshold voltage, μ = mobility, SS = sub-threshold swing

Polymer	I_{on}/I_{off}	V_{TH}(V)	μ(cm^2/V-s)	SS (V/decade)
PTAA	700	−0.15 V to +0.15 V	10^{-2}–10^{-3}	0.37
Polyaniline	2	1.8	10^{-4}	3.70

Abbreviation: PTAA, poly (triaryl amine).

As a simple but important application, the device was tested for binary operation. Figure 6 shows the pulsed response using the electrical circuit schematic shown in the inset. An input ±1.5 V symmetric square wave pulse was applied to the gate terminal, while the drain-source voltage (V_{DS}) was held fixed at either 0 V (red) or −2.0 V (blue). The output voltage was tapped across the load resistor of 10 kΩ. As seen in Figure 6, the response for $V_{DS} = 0$ V is negligible for any input variation as expected. A small transient spike at the rising and falling edges of the input pulse is seen due to capacitive coupling between the gate and the source terminal. The steady state output voltage however is seen to be negligible, confirming that the leakage current (I_{GS}) across the IL/source terminal is insignificant. When $V_{DS} = -2$ V there is a significant output voltage only when the gate is biased negative with respect to the source. This corresponds the "on" state of the device, while during the positive gate cycle the device is "off." Repeatedly cycling the input retains this behavior and demonstrates the suitability of using this device in electronic circuits employing low-operating voltages.

4 | CONCLUSIONS

The electrical performance of a PTAA thin film FET with IL gating in air is reported for the first time. As a result of the high-specific capacitance of the IL, the operating voltages are reduced to a few volts while retaining the high-on/off ratio and hole mobility. This is a significant improvement over other reports that used much higher operating voltages. The device on/off ratio was ∼700 and the mobility was in the range 10^{-2}–10^{-3} cm^2/V-s. When compared to polyaniline, a PTAA based FET has improved device parameters and is a superior semiconducting polymer. The device was successfully tested for binary operation and we demonstrate its suitability for use in low-power consumption electronic circuits.

ACKNOWLEDGMENTS

This work was supported in part by NSF under grants DMR-RUI-1800262 and DMR-PREM-1523463.

ORCID

Nicholas J. Pinto https://orcid.org/0000-0003-0954-6539

REFERENCES

[1] C. K. Chiang, C. R. Fincher Jr., Y. W. Park, A. J. Heeger, H. Shirakawa, E. J. Louis, S. C. Gau, A. G. MacDiarmid, *Phys. Rev. Lett.* **1997**, *39*, 1098.

[2] F. Garnier, R. Hajlaoui, A. Yassar, P. Srivastava, *Science* **1994**, *265*, 1684.

[3] S. R. Forrest, *Nature* **2004**, *428*, 911.

[4] H. Matsui, Y. Takeda, S. Tokito, *Org. Electr.* **2019**, *75*, 105432.

[5] A. J. Heeger, *J. Phys. Chem. B* **2001**, *105*, 8475.

[6] H. Rost, J. Ficker, J. S. Alonso, L. Leenders, I. McCulloch, *Synth. Metals* **2004**, *145*, 83.

[7] S. H. Han, Y. H. Kim, S. H. Lee, M. H. Choi, J. Jang, D. J. Choo, *Org. Electr.* **2008**, *9*, 1040.

[8] J. Veres, S. D. Ogier, S. W. Leeming, D. C. Cupertino, S. M. Khaffaf, *Adv. Func. Mat.* **2003**, *13*, 199.

[9] A. Das, R. Dost, T. Richardson, M. Grell, J. J. Morrison, M. L. Turner, *Adv. Mat.* **2007**, *19*, 4018.

[10] W. Zhang, J. Smith, R. Hamilton, M. Heeney, J. Kirkpatrick, K. Song, S. E. Watkins, T. Anthopoulos, I. McCulloch, *J. Am. Chem. Soc.* **2009**, *131*, 10814.

[11] M. B. Madec, J. J. Morrison, V. Sanchez-Romaguera, M. L. Turner, S. G. Yeates, *J. Mater. Chem.* **2009**, *19*, 6750.

[12] J. Smith, R. Hamilton, I. McCulloch, M. Heeney, J. E. Anthony, D. D. C. Bradley, T. D. Anthopoulos, *Synth. Metals* **2009**, *159*, 2365.

[13] Y. Ko, Y. Kim, C. Lee, Y. Kim, Y. Jun, *ACS Appl. Mater. Interfaces* **2018**, *10*, 11633.

[14] S. G. J. Mathijssen, M. Colle, A. J. G. Mank, M. Kemerink, P. A. Bobbert, D. M. de Leeuw, *Appl. Phys. Lett.* **2007**, *90*, 192104.

[15] L. M. Rijos, A. Melendez, R. Oyola, N. J. Pinto, *Synth. Metals* **2019**, *257*, 116176.

[16] J. Lee, L. G. Kaake, J. H. Cho, X.-Y. Zhu, T. P. Lodge, C. D. Frisbie, *J. Phys. Chem. C* **2009**, *113*, 8972.

[17] C. H. Kim, C. D. Frisbie, *J. Phys. Chem. C* **2014**, *118*, 21160.

[18] A. R. Brown, C. P. Jarrett, D. M. de Leeuw, M. Matters, *Synth. Metals* **1997**, *88*, 37.

[19] J. H. Cho, J. Lee, Y. He, B. S. Kim, T. P. Lodge, C. D. Frisbie, *Adv. Mater.* **2008**, *20*, 686.

[20] L. G. Kaake, Y. Zou, M. J. Panzer, C. D. Frisbie, X. Y. Zhu, *J. Am. Chem. Soc.* **2007**, *129*, 7824.

[21] S. M. Sze, *Physics of Semiconductor Devices*, Wiley, New York **1981**.

[22] R. Dost, A. Das, M. Grell, *Appl. Phys. Lett.* **2008**, *104*, 084519.

[23] D. Braga, I. G. Lezama, H. Berger, A. F. Morpurgo, *Nano Lett.* **2012**, *12*, 5218.

SUPPORTING INFORMATION

Additional supporting information may be found online in the Supporting Information section at the end of this article.

How to cite this article: Rijos LM, Figueroa KS, Porcu A, et al. Ionic liquid gated poly(triaryl amine) thin film field effect transistor. *J Appl Polym Sci*. 2021;138:e50361. https://doi.org/10.1002/app.50361